The Latest Results from PHOBOS: Systematics of Charged Particle Production Through $\sqrt{s_{NN}} = 200$ GeV

Mark D. Baker for the PHOBOS Collaboration:

B.B.Back[1], M.D.Baker[2], D.S.Barton[2], R.R.Betts[6], R.Bindel[7], A.Budzanowski[3], W.Busza[4], A.Carroll[2], J.Corbo[2], M.P.Decowski[4], E.Garcia[6], N.George[1], K.Gulbrandsen[4], S.Gushue[2], C.Halliwell[6], J.Hamblen[8], C.Henderson[4], D.Hicks[2], D.Hofman[6], R.S.Hollis[6], R.Hołyński[3], B.Holzman[2], A.Iordanova[6], E.Johnson[8], J.Kane[4], J.Katzy[4,6], N.Khan[8], W.Kucewicz[6], P.Kulinich[4], C.M.Kuo[5], W.T.Lin[5], S.Manly[8], D.McLeod[6], J.Michałowski[3], A.Mignerey[7], J.Mülmenstädt[4], R.Nouicer[6], A.Olszewski[3], R.Pak[2], I.C.Park[8], H.Pernegger[4], M.Rafelski[2], M.Rbeiz[4], C.Reed[4], L.P.Remsberg[2], M.Reuter[6], C.Roland[4], G.Roland[4], L.Rosenberg[4], J. Sagerer[6], P.Sarin[4], P.Sawicki[3], W.Skulski[8], S.G.Steadman[4], P.Steinberg[2], G.S.F.Stephans[4], M.Stodulski[3], A.Sukhanov[2], J.-L.Tang[5], R.Teng[8], A.Trzupek[3], C.Vale[4], G.J.van Nieuwenhuizen[4], R.Verdier[4], B.Wadsworth[4], F.L.H.Wolfs[8], B.Wosiek[3], K.Woźniak[2,3], A.H.Wuosmaa[1], B.Wysłouch[4]

[1] Physics Division, Argonne National Laboratory, Argonne, IL 60439-4843

[2] Chemistry and C-A Departments, Brookhaven National Laboratory, Upton, NY 11973-5000

[3] Institute of Nuclear Physics, Kraków, Poland

[4] Laboratory for Nuclear Science, Massachusetts Institute of Technology, Cambridge, MA 02139-4307

[5] Department of Physics, National Central University, Chung-Li, Taiwan

[6] Department of Physics, University of Illinois at Chicago, Chicago, IL 60607-7059

[7] Department of Chemistry, University of Maryland, College Park, MD 20742

[8] Department of Physics and Astronomy, University of Rochester, Rochester, NY 14627

(November 6, 2001)

We present the latest results from the PHOBOS collaboration at RHIC, including the first measurement of charged particle production in Au+Au collisions at $\sqrt{s_{NN}} = 200$ GeV. For the 6% most central collisions, we obtain $dN_{ch}/d\eta|_{|\eta|<1} = 650 \pm 35$(syst). Compared to collisions at $\sqrt{s_{NN}} = 130$ GeV, the highest energy studied previously, a modest increase by a factor of 1.14 ± 0.05 is found for pseudorapidity near zero. Away from mid-rapidity, the data are consistent with limiting fragmentation: no energy dependence is seen when the data are plotted as a function of $\eta - y_{beam}$.

Relativistic heavy ion collisions provide a laboratory for studying the strong interaction, described by Quantum Chromodynamics (QCD), under conditions of high parton density and high energy density. This regime is interesting because it probes nonlinear dynamics (e.g. parton saturation), and nonperturbative effects (e.g. the onset of color deconfinement and chiral symmetry restoration). One very simple, but fundamental, heavy ion observable is the pseudorapidity density $dN_{ch}/d\eta$ of charged particles produced in a collision. This number is proportional to the entropy density at freezeout. Since total entropy cannot decrease with time, even in non-equilibrium systems, the pseudorapidity density provides a strong constraint on the initial state parton density and any further entropy produced during the subsequent evolution.

We have measured the pseudorapidity distribution for charged particles, $dN_{ch}/d\eta$, in the most central Au+Au collisions at $\sqrt{s_{NN}} = 200$ GeV. In combination with results from lower energies, these data permit a systematic analysis of particle production mechanisms in nucleus-nucleus collisions. In particular, some models predict an increase in the relative contribution of hard (perturbative) parton-parton scattering processes compared to soft, non-perturbative processes, which in turn leads to a stronger entropy increase.

Details of the PHOBOS experimental setup can be found elsewhere [1,2]. The apparatus, shown schematically in Fig. 1, employs silicon detectors for vertex finding, particle tracking and multiplicity measurements. This analysis is based on the first 6 layers of the 16 layer two-arm spectrometer (SPEC), the two-layer vertex detector (VTX), the single-layer octagon barrel detector (OCT) and the three single-layer ring detectors (RING) located on either side of the interaction point. The acceptance of SPEC and VTX includes $-1 < \eta < 1$, covering different regions of azimuth. The combined acceptance of OCT and RING detectors reaches $\eta = \pm 5.4$. For the 2001 run period, over 100,000 silicon channels were read out, of which more than 98% worked correctly.

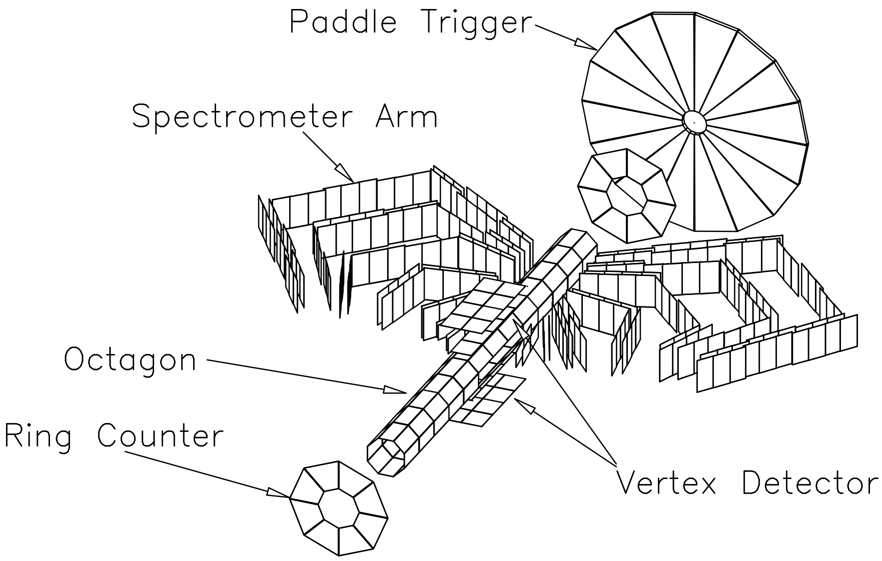

FIG. 1. Schematic diagram of the detector setup for the 2001 running period. Shown are the active elements of the detector systems used for this analysis. For clarity, one of the paddle counters and the two outer ring counters on each side were omitted and the positions of ring and paddle counters are not to scale.

The detector setup also included two sets of 16 scintillator counters ("paddle counters") located at -3.21 m (PN) and $+3.21$ m (PP) relative to the nominal interaction point along the beam (z) axis. These counters covered pseudorapidities between $3 < |\eta| < 4.5$ and served as the primary event trigger. These counters were also used for offline event selection, in combination with timing cuts based on the zero-degree calorimeters at $z = \pm 18.5$ m, which measured the energy deposited by spectator neutrons.

Monte Carlo (MC) simulations of the detector performance were based on the HIJING event generator [3] and the GEANT 3.21 simulation package, folding in the signal response for scintillator counters and silicon sensors. In the calibration of the analysis methods we employed a particle selection procedure that allowed us to iteratively modify the MC output and optimize the agreement of the deposited energy distributions in data and MC.

Details of the trigger performance, the event selection procedure, and the vertex finding procedure can be found in [4,5]. We selected the top 6% of the total hadronic cross section with the largest combined signal from PP and PN ("paddle mean"), corresponding to the most central collisions with the largest number of participating nucleons. Applying the 6% centrality cut to MC events, we deduce that the average number of participating nucleons in the data is $\langle N_{part} \rangle = 344 \pm 10$ (syst) for $\sqrt{s_{_{NN}}} = 200$ GeV, 343 ± 10 (syst) for 130 GeV, and 330 ± 10 (syst.) for 56 GeV.

The analysis leading to the charged particle pseudorapidity density measurement is described in a recent publication [6], using methods developed and described in detail in previous publications [4,5,7]. The multiplicity densities $dN_{ch}/d\eta$ were corrected for particles which stop in the material of the beam pipe and the first detector layer, particles from secondary interactions and feed-down products from weak decays of neutral strange particles. The resulting systematic errors for each method at $\sqrt{s_{_{NN}}} = 130$ GeV and 200 GeV are described in [4–7] and range from 4.5% to 10%, independent of energy, but depending on method. The combined result of all four methods is obtained using the inverse square of the estimated uncertainties as weights in the average. Based on MC studies and the comparison of all four independent multiplicity analyses, we estimate the overall systematic uncertainty of the combined result to be less than 6%. The statistical error is negligible. We obtain a primary charged particle density of $dN_{ch}/d\eta|_{|\eta|<1} = 650 \pm 35$(syst) for the 6% most central Au+Au collisions at $\sqrt{s_{_{NN}}} = 200$ GeV. Normalizing per participant pair, we find $dN_{ch}/d\eta|_{|\eta|<1}/\langle \frac{1}{2} N_{part} \rangle = 3.78 \pm 0.25$(syst).

Early predictions for the charged particle pseudorapidity density varied by more than a factor of two, as shown in [8]. Data on the primary charged particle density $dN_{ch}/d\eta|_{|\eta|<1}$ at energies of $\sqrt{s_{_{NN}}} = 56$ and 130 GeV [4] showed that the entropy was at the low end of the expected range, constraining the theoretical models and leading to a much narrower range of new predictions [9–17]. Generally, most models allowed a reasonable description of the energy dependence of $dN_{ch}/d\eta|_{|\eta|<1}$ up to $\sqrt{s_{_{NN}}} = 130$ GeV, with suitable choices of parameters. For the ratio of particle densities near $\eta = 0$ at 130 GeV and 200 GeV, the calculations predict an increase between 9 and 31%. It is instructive to examine the extremes. The model with the largest prediction uses default HIJING, by Wang and Gyulassy [9]. In this model, jet quenching effects are assumed to be large and, furthermore, all of the gluon radiation is assumed to lead to new particle production rather than thermal interactions. This leads to an increase of mid-rapidity multiplicity of more than 30% between 130 and 200 GeV. Even when jet quenching is turned completely off, the large amount of hard scattering ("minijet production") in HIJING leads to an increase of more than 20%. Similarly, the "soft+hard" model of Kharzeev and Levin [10] produces a 20% increase. The four models with the lowest predictions (other than simple $p\bar{p}$ extrapolation) involve mechanisms which limit hard scattering and keep the entropy down: strings [15,17], purely hadronic cascade [16], or Kharzeev-Levin parton saturation [10].

A compilation of all results for $dN_{ch}/d\eta\rfloor_{|\eta|<1}/\langle\frac{1}{2}N_{part}\rangle$ in central Au+Au collisions obtained at RHIC can be found in reference [6], including results from PHOBOS at $\sqrt{s_{NN}}$ = 56 GeV, from all four RHIC experiments at $\sqrt{s_{NN}}$ = 130 GeV [4,5,7,18–20] and the new PHOBOS result at $\sqrt{s_{NN}}$ = 200 GeV. The average value for all RHIC data at 130 GeV is $dN_{ch}/d\eta\rfloor_{|\eta|<1}/\langle\frac{1}{2}N_{part}\rangle = 3.37 \pm 0.12$, compared to 3.78 ± 0.25 reported here for 200 GeV. In Fig. 2 the normalized yield per participant is compared to central Au+Au and Pb+Pb collisions at lower energy, fixed target, experiments [21–23]. Also shown for comparison are results from proton-antiproton ($p\overline{p}$) collisions [24] and an interpolation of the $p\overline{p}$ data. The $dN_{ch}/d\eta$ values from E866/E917 [21] and NA49 [22,23] were obtained by integrating the measured charged particle rapidity and p_T-distributions. Within the precision of the existing data, an approximately logarithmic rise of $dN_{ch}/d\eta|_{|\eta|<1}/\langle\frac{1}{2}N_{part}\rangle$ with $\sqrt{s_{NN}}$ is observed over the full range of collision energies.

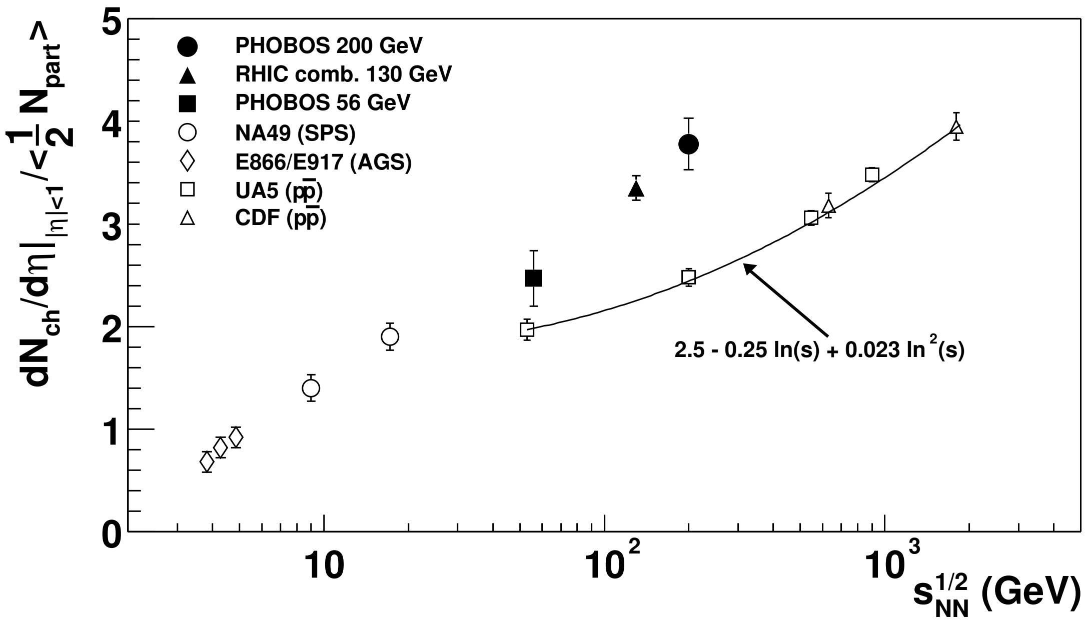

FIG. 2. Energy dependence of the pseudorapidity density normalized per participant pair for central nucleus-nucleus collisions. The data are compared with $p\overline{p}$ data and nucleus-nucleus data from lower energies.

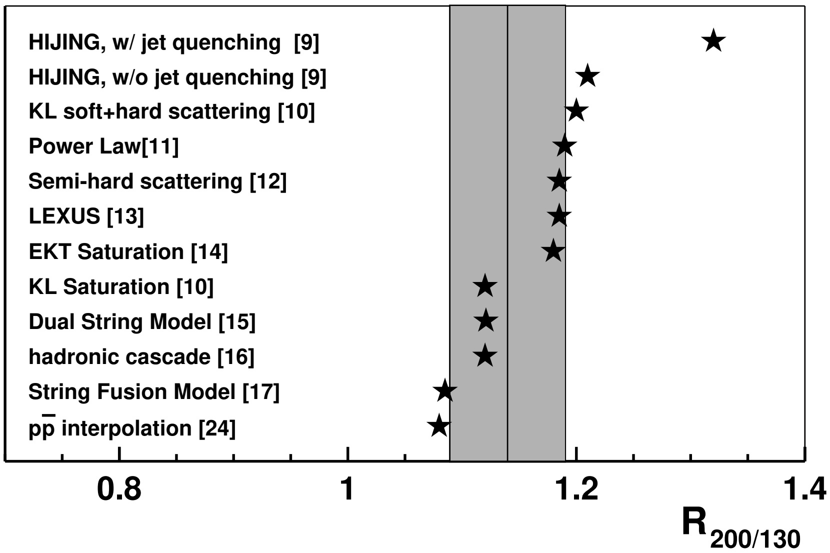

FIG. 3. Ratio $R_{200/130}$ of pseudorapidity densities $dN_{ch}/d\eta|_{|\eta|<1}$ at $\sqrt{s_{NN}}$ = 200 GeV and 130 GeV. The predicted increase from various models is compared to the observed increase in the data (vertical line). The grey band shows the 90% confidence interval.

The ratio $R_{200/130}$ of normalized multiplicity densities $dN_{ch}/d\eta|_{|\eta|<1}/\langle\frac{1}{2}N_{part}\rangle$ at $\sqrt{s_{NN}}$ = 200 GeV and 130 GeV can be determined directly in our experiment. This has the advantage of allowing some systematic errors to cancel in the ratio as described in [6]. The final result, based on an average of four different methods, is $R_{200/130} = 1.14 \pm 0.05$. The quoted uncertainty is entirely systematic and corresponds to a 90% confidence level. In Fig. 3 this value is compared with the $p\bar{p}$ parameterization [24] and several model calculations. The expected increase from the interpolation of $p\bar{p}$ results falls slightly below the allowed region. The energy dependence of particle production presented here, showing only a modest growth with energy, provides important constraints on entropy production. Specifically, this rules out the default version of HIJING and strongly disfavors the next two models shown: HIJING with no jet quenching and the soft+hard model discussed by Kharzeev and Levin. More generally, this result limits the amount of particle production from hard scattering and gluon radiation (jet quenching).

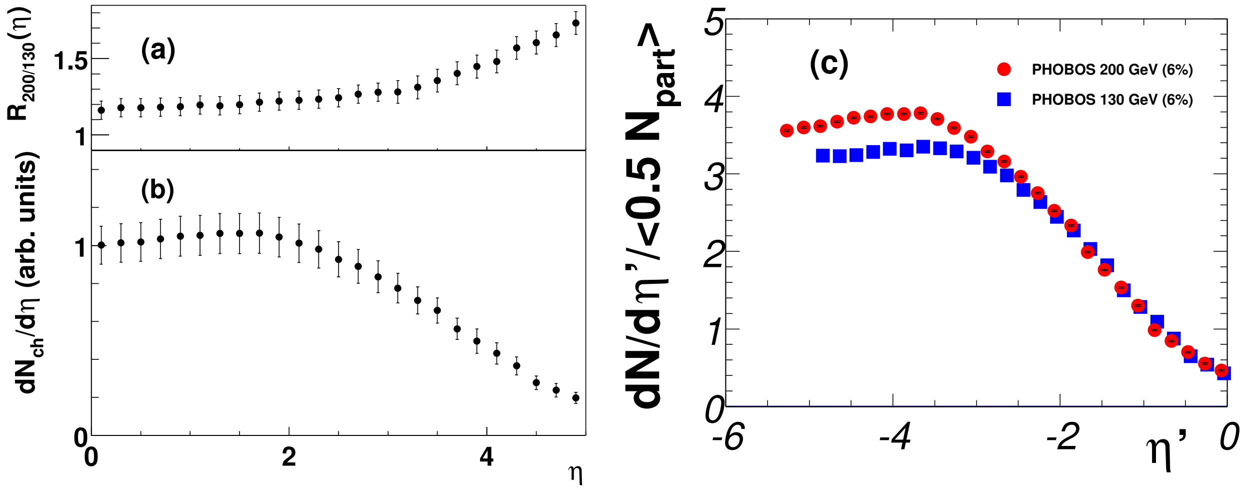

FIG. 4. Panel b) shows the shape of $dN_{ch}/d\eta$ at $\sqrt{s_{NN}}$ = 200 GeV, obtained from the analog method, normalized to $dN_{ch}/d\eta|_{\eta=0}$. Panel a) shows the pseudorapidity dependence of $R_{200/130}$ using the result of the analog method at both energies. In both a) and b), the error bars indicate the systematic uncertainty at the 90% C.L. Panel c) shows the same data plotted as $dN_{ch}/d\eta'$ per participant pair, where $\eta' \equiv \eta - y_{beam}$ for $Au+Au$ collisions at $\sqrt{s_{NN}}$ = 130 and 200 GeV. Like the $p+\bar{p}$ data [26], the PHOBOS data shows evidence for limiting fragmentation, defined as the energy independence of the momentum distribution in the target frame, away from mid-rapidity in the cm frame. NOTE: Systematic errors are not shown in panel c).

Additional information about the change in particle production from 130 GeV to 200 GeV collision energy can be gained from Fig. 4. Using the results from the analog method alone [7], it shows $dN_{ch}/d\eta$ out to $\eta = 5$ for central collisions at 200 GeV (panel b) and the ratio of the pseudorapidity distributions at 200 and 130 GeV (panel a). A slow increase of the ratio is observed to $\eta \approx 3$. This is followed by a steeper rise at higher η, corresponding to a widening of the pseudorapidity distribution and reflecting the shift in the fragmentation region due to the larger beam rapidity at 200 GeV.

In order to illuminate this situation further, let us consider particle production away from mid-rapidity in the beam (or target) rest frame. The distributions, $d^2N_{ch}/dy'dp_T$, of charged particles from $p+p$ and $p+\bar{p}$ collisions have been shown to be energy-independent near $y' = 0$ as predicted by the "limiting fragmentation" hypothesis [25,26], where $y' \equiv y - y_{beam}$ and y is the rapidity in the center-of-mass frame. A similar relationship holds for $y - y_{targ.}$. Away from midrapidity, we can can approximate $e^y \approx 2\cosh y \approx 2\sinh y$ and $e^\eta \approx 2\cosh\eta \approx 2\sinh\eta$. This allows us to write $y - y_{beam} = \ln x_F^+ + \ln(M_N/m_T)$ where $x_F^+ \equiv (E+p_z)/(E+p_z)_{max}$ is the light-cone version of Feynman x for the charged particles, $m_T \equiv \sqrt{p_T^2 + m^2}$ is the transverse mass for the charged particles, M_N is the M/A of the nucleus, and $\sqrt{s_{_{NN}}}$ is the NN cm energy. Experimentally, it is more straightforward to use the variable $\eta' \equiv \eta - y_{beam}$, which we can write as

$$\eta' \equiv \eta - y_{beam} = \ln x_F^+ + \ln(M_N/p_T),$$

For a given p_T, this variable is related to the more intuitive $y - y_{beam} = \ln x_F^+ + \ln(M_N/m_T)$ by a constant shift: $\ln(p_T/m_T)$.

Figure 4c shows the results for $Au+Au$ collisions at $\sqrt{s_{_{NN}}}$ of 130 and 200 GeV, showing good agreement over more than 2 units of η'. This measurement shows that limiting fragmentation works well in the $Au+Au$ system. It should be noted that the hypothesis of limiting fragmentation does not, in itself, imply that the $p+\bar{p}$ and $Au+Au$ data must agree with each other, just that each should reach a limiting value for $dN/d\eta'$ as the energy increases.

Figure 5 shows the centrality dependence of $dN/d\eta$, measured over 11 units of pseudorapidity. See reference [7] for the systematic errors on this data, which are not shown in this plot. This result shows that the "fragmentation region" behavior changes significantly with centrality. For $\eta > 3.5$, the normalized multiplicity density actually grows in the peripheral data with respect to the more central data. Data on $p+A$ collisions [27] suggest two possible explanations for this. First, in the projectile (proton) rest frame, increasing A results in a shift of the projectile towards midrapidity. In $A+A$ collisions this could decrease the $dN/d\eta$ at large η in central collisions. Second, in the $p+A$ target (nucleus) rest frame, near $y = 0$, the scaled density: $dN/dy/\langle\bar{\nu}\rangle$ increases with increasing A, where $\langle\bar{\nu}\rangle$ is the "number of collisions" or the estimated average number of nucleons in the target (A) which are struck by the incoming proton p. This means that the number of charged particles in the final state grows faster than the number of participating target nucleons, implying that the "spectator" matter also contributes to particle production in the target fragmentation region. In $p+A$ physics, this is known as intranuclear cascading. Intranuclear cascading should also show up as an increase in particles produced at large y or η in peripheral AA collisions compared to central AA collisions, as seen in Figure 5.

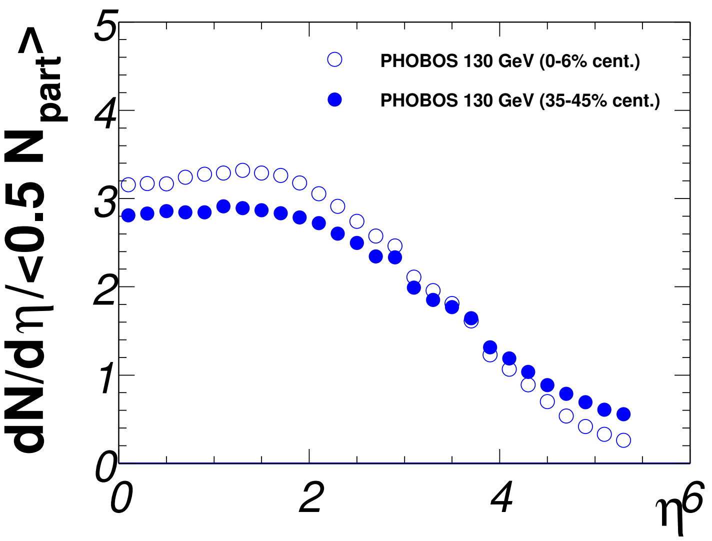

FIG. 5. Normalized multiplicity density $dN_{ch}/d\eta/\langle\frac{1}{2}N_{part}\rangle$ at $\sqrt{s_{_{NN}}}$ = 130 GeV for central (0-6%, open symbols) and mid-central (35-45%, filled symbols) collisions. NOTE: Systematic errors are not shown.

Additional measurements made by PHOBOS during the last year at $\sqrt{s_{_{NN}}}$ = 130 GeV include particle ratios at midrapidity [28] and a preliminary measurement of elliptic flow over a broad range of pseudorapidity [29]. The particle ratios show that the system is significantly more baryon free than at lower energies. The elliptic flow shows a surprising strength compared to lower energies at midrapidity and the preliminary indication is that there may be a non-trivial η dependence.

In summary, we have examined $Au+Au$ collisions at RHIC energies, performing the only measurement at $\sqrt{s_{_{NN}}}$ = 56 GeV, several measurements at $\sqrt{s_{_{NN}}}$ = 130 GeV, and the first measurement of the pseudorapidity density of primary charged particles in Au+Au collisions at $\sqrt{s_{_{NN}}}$ = 200 GeV. Near mid-rapidity, this density shows an approximately logarithmic evolution over a broad range of collision energies. Going from $\sqrt{s_{_{NN}}}$ = 130 GeV to 200 GeV, the observed increase is a factor of 1.14 ± 0.05, corresponding to a moderate increase in initial energy density. Over this energy interval, a smooth evolution of $dN_{ch}/d\eta$ in all regions of pseudorapidity is seen. This implies a modest increase in entropy compared to the original range of expectations, providing serious constraints for models: only a limited amount of entropy is allowed in the initial state and significant entropy generation during the subsequent evolution is basically ruled out. Furthermore, this entropy increase was shown to be concentrated at mid-rapidity as $dN/d\eta'$ ($\eta' \equiv \eta - y_{beam}$) was energy-independent from 130 to 200 GeV over a broad range of $-2 < \eta' < 0$ (limiting fragmentation).

Acknowledgements: This work was partially supported by US DoE grants DE-AC02-98CH10886, DE-FG02-93ER40802, DE-FC02-94ER40818, DE-FG02-94ER40865, DE-FG02-99ER41099, W-31-109-ENG-38. NSF grants 9603486, 9722606 and 0072204. The Polish groups were partially supported by KBN grant 2 P03B 04916. The NCU group was partially supported by NSC of Taiwan under contract NSC 89-2112-M-008-024.

[1] B. B. Back *et al.*, Nucl. Phys. **A661** (1999) 690.
[2] H. Pernegger *et al.*, Nucl. Instrum. Methods. **A419** (1998) 549.
[3] M. Gyulassy and X. N. Wang, Phys. Rev. **D44** (1991) 3501.
[4] B. B. Back *et al.*, Phys. Rev. Lett. **85** (2000) 3100.
[5] B. B. Back *et al.*, nucl-ex/0105011.
[6] B. B. Back *et al.*, Phys. Rev. Lett. in press, nucl-ex/0108009.
[7] B. B. Back *et al.*, Phys. Rev. Lett. **87** (2001) 102303.
[8] N. Armesto and C. Pajares, Int. J. Mod. Phys. **A15** (2000) 2019.
[9] X. N. Wang and M. Gyulassy, Phys. Rev. Lett. **86** (2001) 3496.
[10] D. Kharzeev and E. Levin, nucl-th/0108066 (2001).
[11] S. Barshay and G. Kreyerhoff, hep-ph/0104303 (2001).
[12] A. Accardi, hep-ph/0104060 (2001).
[13] S. Jeon and J. Kapusta, Phys. Rev. C **63** (2001) 011901.
[14] K. J. Eskola *et al.*, hep-ph/0106330 (2001).
[15] J. Dias de Deus and R. Ugoccioni, Phys. Lett. **B491** (2000) 253.
[16] D. E. Kahana and S. H. Kahana, Phys. Rev. C **63** (2001) 031901(R).
[17] N. Armesto, C. Pajares and D. Sousa, hep-ph/0104269 (2001).
[18] K. Adcox *et al.*, Phys. Rev. Lett. **86** (2001) 3500.
[19] F. Videbaek *et al.*, Proceedings of QM 2001 conference, in press.
[20] C. Adler *et al.*, Phys. Rev. Lett. bf 87 (2001) 112303.
[21] L. Ahle *et al.*, Phys. Lett. B **476**, (2000) 1; L. Ahle *et al.*, Phys. Lett. B **490** (2000) 53; B. B. Back *et al.*, Phys. Rev. Lett. **86**, (2001) 1970.
[22] J. Bächler *et al.*, Nucl. Phys. **A661** (1999) 45.
[23] C. Blume *et al.*, Proceedings of QM 2001 conference, in press.
[24] F. Abe *et al.*, Phys. Rev. **D41** (1990) 2330.
[25] J. Benecke, T. T. Chou, C-N. Yang, E. Yen, Phys. Rev. 188 (1969) 2159.
[26] UA5 Collaboration, Z. Phys. **C33** (1986) 1.
[27] deMarzo et al., Phys. Rev. D **26** (1982) 1019.
[28] B. B. Back *et al.*, Phys. Rev. Lett. **87** (2001) 102301.
[29] I. C. Park *et al.*, Proceedings of QM2001 conference, in press.